Phonons in Nanostructures

Michael A. Stroscio and Mitra Dutta
US Army Research Office, US Army Research Laboratory

CAMBRIDGE
UNIVERSITY PRESS

PUBLISHED BY THE PRESS SYNDICATE OF THE UNIVERSITY OF CAMBRIDGE
The Pitt Building, Trumpington Street, Cambridge, United Kingdom

CAMBRIDGE UNIVERSITY PRESS
The Edinburgh Building, Cambridge CB2 2RU, UK
40 West 20th Street, New York, NY 10011-4211, USA
10 Stamford Road, Oakleigh, VIC 3166, Australia
Ruiz de Alarcón 13, 28014, Madrid, Spain
Dock House, The Waterfront, Cape Town 8001, South Africa

http://www.cambridge.org

First published 2001

Printed in the United Kingdom at the University Press, Cambridge

Typeface Times 10.25/13.5pt. *System* LaTeX 2$_\varepsilon$ [DBD]

A catalogue record of this book is available from the British Library

Library of Congress Cataloguing in Publication data

Stroscio, Michael A., 1949–
Phonons in nanostructures / Michael A. Stroscio and Mitra Dutta.
p. cm.
Includes bibliographic references and index.
ISBN 0 521 79279 7
1. Nanostructures. 2. Phonons. I. Dutta, Mitra. II. Title.

QC176.8.N35 S77 2001
530.4′16–dc21 00-54669

ISBN 0 521 79279 7 hardback

Contents

Chapter 1

Phonons in nanostructures

There are no such things as applied sciences, only applications of sciences.
Louis Pasteur, 1872

1.1 Phonon effects: fundamental limits on carrier mobilities and dynamical processes

The importance of phonons and their interactions in bulk materials is well known to those working in the fields of solid-state physics, solid-state electronics, optoelectronics, heat transport, quantum electronics, and superconductivity.

As an example, carrier mobilities and dynamical processes in polar semiconductors, such as gallium arsenide, are in many cases determined by the interaction of longitudinal optical (LO) phonons with charge carriers. Consider carrier transport in gallium arsenide. For gallium arsenide crystals with low densities of impurities and defects, steady state electron velocities in the presence of an external electric field are determined predominantly by the rate at which the electrons emit LO phonons. More specifically, an electron in such a polar semiconductor will accelerate in response to the external electric field until the electron's energy is large enough for the electron to emit an LO phonon. When the electron's energy reaches the threshold for LO phonon emission – 36 meV in the case of gallium arsenide – there is a significant probability that it will emit an LO phonon as a result of its interaction with LO phonons. Of course, the electron will continue to gain energy from the electric field.

In the steady state, the processes of electron energy loss by LO phonon emission and electron energy gain from the electric field will come into balance and the electron will propagate through the semiconductor with a velocity known as the saturation velocity. As is well known, experimental values for this saturated drift velocity generally fall in the range 10^7 cm s^{-1} to 10^8 cm s^{-1}. For gallium arsenide this velocity is about 2×10^7 cm s^{-1} and for indium antimonide 6×10^7 cm s^{-1}.

For both these polar semiconductors, the process of LO phonon emission plays a major role in determining the value of the saturation velocity. In non-polar materials such as Si, which has a saturation velocity of about 10^7 cm s^{-1}, the deformation-potential interaction results in electron energy loss through the emission of phonons. (In Chapter 5 both the interaction between polar-optical-phonons and electrons – known as the Fröhlich interaction – and the deformation-potential interaction will be defined mathematically.)

Clearly, in all these cases, the electron mobility will be influenced strongly by the interaction of the electrons with phonons. The saturation velocity of the carriers in a semiconductor provides a measure of how fast a microelectronic device fabricated from this semiconductor will operate. Indeed, the minimum time for the carriers to travel through the active region of the device is given approximately by the length of the device – that is, the length of the so-called gate – divided by the saturation velocity. Evidently, the practical switching time of such a microelectronic device will be limited by the saturation velocity and it is clear, therefore, that phonons play a major role in the fundamental and practical limits of such microelectronic devices. For modern integrated circuits, a factor of two reduction in the gate length can be achieved in many cases only through building a new fabrication facility. In some cases, such a building project might cost a billion dollars or more. The importance of phonons in microelectronics is clear!

A second example of the importance of carrier–phonon interactions in modern semiconductor devices is given by the dynamics of carrier capture in the active quantum-well region of a polar semiconductor quantum-well laser. Consider the case where a current of electrons is injected over a barrier into the quantum-well region of such a laser. For the laser to operate, an electron must lose enough energy to be 'captured' by the quasi-bound state which it must occupy to participate in the lasing process. For many quantum-well semiconductor lasers this means that the electron must lose an energy of the order of a 100 meV or more. The energy loss rate of a carrier – also known as the thermalization rate of the carrier – in a polar-semiconductor quantum well is determined by both the rate at which the carrier's energy is lost by optical-phonon emission and the rate at which the carrier gains energy from optical-phonon absorption. This latter rate can be significant in quantum wells since the phonons emitted by energetic carriers can accumulate in these structures. Since the phonon densities in many dimensionally confined semiconductor devices are typically well above those of the equilibrium phonon population, there is an appreciable probability that these non-equilibrium – or 'hot' – phonons will be reabsorbed. Clearly, the net loss of energy by an electron in such a situation depends on the rates for both phonon absorption and phonon emission. Moreover, the lifetimes of the optical phonons are also important in determining the total energy loss rate for such carriers. Indeed, as will be discussed in Chapter 6, the longitudinal optical (LO) phonons in GaAs and many other polar materials decay into acoustic phonons through the Klemens' channel. Furthermore, over a wide

range of temperatures and phonon wavevectors, the lifetimes of longitudinal optical phonons in GaAs vary from a few picoseconds to about 10 ps (Bhatt *et al.*, 1994). (Typical lifetimes for other polar semiconductors are also of this magnitude.) As a result of the Klemens' channel, the 'hot' phonons decay into acoustic phonons in times of the order of 10 ps. The LO phonons undergoing decay into acoustic phonons are not available for absorption by the electrons and as a result of the Klemens' channel the electron thermalization is more rapid than it would be otherwise; this phenomenon is referred to as the 'hot-phonon-bottleneck effect'.

The electron thermalization time is an important parameter for semiconductor quantum-well lasers because it determines the minimum time needed to switch the laser from an 'on' state to an 'off' state; this occurs as a result of modulating the electron current that leads to lasing. Since the hot-phonon population frequently decays on a time scale roughly given by the LO phonon decay rate (Das Sarma *et al.*, 1992), a rough estimate of the electron thermalization time – and therefore the minimum time needed to switch the laser from an 'on' state to an 'off' state – is of the order of about 10 ps. In fact, typical modulation frequencies for gallium arsenide quantum-well lasers are about 30 GHz. The modulation of the laser at significantly higher frequencies will be limited by the carrier thermalization time and ultimately by the lifetime of the LO phonon. The importance of the phonon in modern optoelectronics is clear.

The importance of phonons in superconductors is well known. Indeed, the Bardeen–Cooper–Schrieffer (BCS) theory of superconductivity is based on the formation of bosons from pairs of electrons – known as Cooper pairs – bound through the mediating interaction produced by phonons. Many of the theories describing the so-called high-critical-temperature superconductors are not based on phonon-mediated Cooper pairs, but the importance of phonons in many superconductors is of little doubt. Likewise, it is generally recognized that acoustic phonon interactions determine the thermal properties of materials.

These examples illustrate the pervasive role of phonons in bulk materials. Nanotechnology is providing an ever increasing number of devices and structures having one, or more than one, dimension less than or equal to about 100 ångstroms. The question naturally arises as to the effect of dimensional confinement on the properties on the phonons in such nanostructures as well as the properties of the phonon interactions in nanostructures. The central theme of this book is the description of the optical and acoustic phonons, and their interactions, in nanostructures.

1.2 Tailoring phonon interactions in devices with nanostructure components

Phonon interactions are altered unavoidably by the effects of dimensional confinement on the phonon modes in nanostructures. These effects exhibit some similarities

to those for an electron confined in a quantum well. Consider the well-known wavefunction of an electron in an infinitely deep quantum well, of width L_z in the z-direction. The energy eigenstates $\Psi_n(z)$ may be taken as plane-wave states in the directions parallel to the heterointerfaces and as bound states in an infinitely deep quantum well in the z-direction:

$$\Psi_n(z) = \frac{e^{i\mathbf{k}_\parallel \cdot \mathbf{r}_\parallel}}{\sqrt{A}} \sqrt{\frac{2}{L_z}} \sin k_z z, \tag{1.1}$$

where $\mathbf{r}_\parallel$ and $\mathbf{k}_\parallel$ are the position vector and wavevector components in a plane parallel to the interfaces, $k_z = n\pi/L_z$, and $n = 1, 2, 3, \ldots$ labels the energy eigenstates, whose energies are

$$E_n(\mathbf{k}_\parallel) = \frac{\hbar^2(\mathbf{k}_\parallel)^2}{2m} + \frac{\hbar^2\pi^2 n^2}{2mL_z^2}. \tag{1.2}$$

A is the area of the heterointerface over which the electron wavefunction is normalized. Clearly, a major effect of dimensional confinement in the z-direction is that the z-component of the bulk continuum wavevector is restricted to integral multiples of π/L_z. Stated in another way, the phase space is restricted.

As will be explained in detail in Chapter 7, the dimensional confinement of phonons results in similar restrictions in the phase space of the phonon wavevector q. Indeed, we shall show that the wavevectors of the optical phonons in a dielectric layer of thickness L_z are given by $q_z = n\pi/L_z$ (Fuchs and Kliewer, 1965) in analogy to the case of an electron in an infinitely deep quantum well. In fact, Fasol *et al.* (1988) used Raman scattering techniques to show that the wavevectors $q_z = n\pi/L_z$ of optical phonons confined in a ten-monolayer-thick AlAs/GaAs/AlAs quantum well are so sensitive to changes in L_z that a one-monolayer change in the thickness of the quantum well is readily detectable as a change in q_z! These early experimental studies of Fasol *et al.* (1988) demonstrated not only that phonons are confined in nanostructures but also that the measured phonon wavevectors are well described by relatively simple continuum models of phonon confinement.

Since dimensional confinement of phonons restricts the phase space of the phonons, it is certain that carrier–phonon interactions in nanostructures will be modified by phonon confinement. As we shall see in Chapter 7, the so-called dielectric and elastic continuum models of phonons in nanostructures may be applied to describe the deformation-potential, Fröhlich, and piezoelectric interactions in a variety of nanostructures including quantum wells, quantum wires, and quantum dots. These interactions play a dominant role in determining the electronic, optical and acoustic properties of materials (Mitin *et al.*, 1999; Dutta and Stroscio, 1998b; Dutta and Stroscio, 2000); it is clearly desirable for models of the properties of nanostructures to be based on an understanding of how the above-mentioned interactions change as a result of dimensional confinement. To this end, Chapters

8, 9 and 10 of this book describe how the dimensional confinement of phonons in nanostructures leads to modifications in the electronic, optical, acoustic, and superconducting properties of selected devices and structures, including intersubband quantum-well semiconductor lasers, double-barrier quantum-well diodes, thin-film superconductors, and the thin-walled cylindrical structures found in the biological structures known as microtubulin. Chapters 8, 9, and 10 also provide analyses of the role of collective effects and non-equilibrium phonons in determining hot-carrier energy loss in polar quantum wires as well as the use of metal–semiconductor structures to tailor carrier–phonon interactions in nanostructures. Moreover, Chapter 10 describes how confined phonons play a critical role in determining the properties of electronic, optical, and superconducting devices containing nanostructures as essential elements. Examples of such phonon effects in nanoscale devices include: phonon effects in intersubband lasers; the effect of confined phonons on the gain of intersubband lasers; the contribution of confined phonons to the valley current in double-barrier quantum-well structures; phonon-enhanced population inversion in asymmetric double-barrier quantum-well lasers; and confined phonon effects in thin film superconductors.

Chapter 2

Phonons in bulk cubic crystals

The Creator, if He exists, has a special preference for beetles.
J.B.S. Haldane, 1951

2.1 Cubic structure

Crystals with cubic structure are of major importance in the fields of electronics and optoelectronics. Indeed, zincblende crystals such as silicon, germanium, and gallium arsenide may be regarded as two face-centered cubic (fcc) lattices displaced relative to each other by a vector $(a/4, a/4, a/4)$, where a is the size of the smallest unit of the fcc structure. Figure 2.1 shows a lattice with the zincblende structure.

A major portion of this book will deal with phonons in cubic crystals. In addition, we will describe the phonons in so-called isotropic media, which are related mathematically to cubic media as explained in detail in Section 7.2. The remaining portions of this book will deal with crystals of würtzite structure, defined in Chapter 3. More specifically, the primary focus of this book concerns phonons in crystalline structures that are dimensionally confined in one, two, or three dimensions. Such one-, two-, and three-dimensional confinement is realized in quantum wells, quantum wires, and quantum dots, respectively. As a preliminary to considering phonons in dimensionally confined structures, the foundational case of phonons in bulk structures will be treated. The reader desiring to supplement this chapter with additional information on the basic properties of phonons in bulk cubic materials will find excellent extended treatments in a number of texts including Blakemore (1985), Ferry (1991), Hess (1999), Kittel (1976), Omar (1975), and Singh (1993).

2.2 Ionic bonding – polar semiconductors

As is well known, the crystal structure of silicon is the zincblende structure shown in Figure 2.1. The covalent bonding in silicon does not result in any net transfer of charge between silicon atoms. More specifically, the atoms on the two displaced

face-centered cubic (fcc) lattices depicted in Figure 2.1 have no excess or deficit of charge relative to the neutral situation. This changes dramatically for polar semiconductors like gallium arsenide, since here the ionic bonding results in charge transfer from the Group V arsenic atoms to the Group III gallium atoms: Since Group V atoms have five electrons in the outer shell and Group III atoms have three electrons in the outer shell, it is not surprising that the gallium sites acquire a net negative charge and the arsenic sites a net positive charge. In binary polar semiconductors, the two atoms participating in the ionic bonding carry opposite charges, e^* and $-e^*$, respectively, as a result of the redistribution of the charge associated with polar bonding. In polar materials such ionic bonding is characterized by values of e^* within an order of magnitude of unity. In the remaining sections of this chapter, it will become clear that e^* is related to the readily measurable or known ionic masses, phonon optical frequencies, and high-frequency dielectric constant of the polar semiconductor.

2.3 Linear-chain model and macroscopic models

The linear-chain model of a one-dimensional diatomic crystal is based upon a system of two atoms with masses, m and M, placed along a one-dimensional chain as depicted in Figure 2.2. As for a diatomic lattice, the masses are situated alternately along the chain and their separation is a. On such a chain the displacement of one atom from its equilibrium position will perturb the positions of its neighboring atoms.

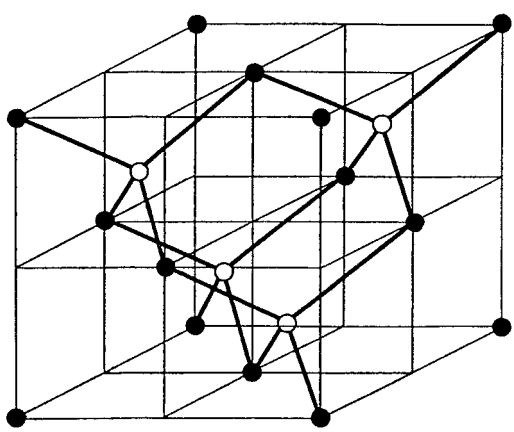

Figure 2.1. Zincblende crystal. The white spheres and black spheres lie on different fcc lattices.

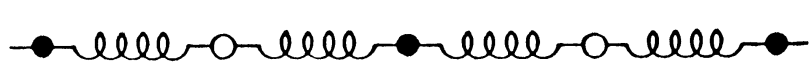

Figure 2.2. One-dimensional linear-chain representation of a diatomic lattice.

In the simple linear-chain model considered in this section, it is assumed that only nearest neighbors are coupled and that the interaction between these atoms is described by Hooke's law; the spring constant α is taken to be that of a harmonic oscillator. This model describes many of the basic properties of a diatomic lattice. However, as will become clear in Chapter 6, it is essential to supplement the so-called 'harmonic' interactions with anharmonic interactions in order to describe the important process of phonon decay.

2.3.1 Dispersion relations for high-frequency and low-frequency modes

To model the normal modes of this system of masses, the atomic displacements along the direction of the chain – the so-called longitudinal displacements of each of the two types of atoms – are taken to be

$$u_{2r} = A_1 e^{i(2rqa-\omega t)} \tag{2.1}$$

and

$$u_{2r+1} = A_2 e^{i[(2r+1)qa-\omega t]} \tag{2.2}$$

where q is the phonon wavevector and ω is its frequency. In the nearest-neighbor approximation, these longitudinal displacements satisfy

$$\begin{aligned} m(d^2u_{2r}/dt^2) &= -\alpha(u_{2r} - u_{2r-1}) - \alpha(u_{2r} - u_{2r+1}) \\ &= \alpha(u_{2r+1} + u_{2r-1} - 2u_{2r}) \end{aligned} \tag{2.3}$$

and

$$\begin{aligned} M(d^2u_{2r+1}/dt^2) &= -\alpha(u_{2r+1} - u_{2r}) - \alpha(u_{2r+1} - u_{2r+2}) \\ &= \alpha(u_{2r+2} + u_{2r} - 2u_{2r+1}). \end{aligned} \tag{2.4}$$

The signs in the four terms on the right-hand sides of these equations are determined by considering the relative displacements of neighboring atoms. For example, if the positive displacement of u_{2r} is greater than that of u_{2r-1} there is a restoring force $-\alpha(u_{2r+1} - u_{2r})$. Hence

$$-m\omega^2 A_1 = \alpha A_2(e^{iqa} + e^{-iqa}) - 2\alpha A_1 \tag{2.5}$$

and

$$-M\omega^2 A_2 = \alpha A_1(e^{iqa} + e^{-iqa}) - 2\alpha A_2. \tag{2.6}$$

Eliminating A_1 and A_2,

$$\omega^2 = \alpha\left(\frac{1}{m} + \frac{1}{M}\right) \pm \alpha\left[\left(\frac{1}{m} + \frac{1}{M}\right)^2 - \frac{4\sin^2 qa}{mM}\right]^{1/2}. \tag{2.7}$$

This relationship between frequency and wavevector is commonly called a dispersion relation. The higher-frequency solution is known as the optical mode

since, for many semiconductors, its frequency is in the terahertz range, which happens to coincide with the infrared portion of the electromagnetic spectrum. The lower-frequency solution is known as the acoustic mode. More precisely, since only longitudinal displacements have been modeled, these two solutions correspond to the longitudinal optical (LO) and longitudinal acoustic (LA) modes of the linear-chain lattice. Clearly, the displacements along this chain can be described in terms of wavevectors q in the range from $-\pi/2a$ to $\pi/2a$. From the solution for ω, it is evident that over this Brillouin zone the LO modes have a maximum frequency $[2\alpha(1/m + 1/M)]^{1/2}$ at the center of the Brillouin zone and a minimum frequency $(2\alpha/m)^{1/2}$ at the edge of the Brillouin zone. Likewise, the LA modes have a maximum frequency $(2\alpha/M)^{1/2}$ at the edge of the Brillouin zone and a minimum frequency equal to zero at the center of the Brillouin zone.

In polar semiconductors, the masses m and M carry opposite charges, e^* and $-e^*$, respectively, as a result of the redistribution of the charge associated with polar bonding. In polar materials such ionic bonding is characterized by values of e^* equal to 1, to an order-of-magnitude. When there is an electric field E present in the semiconductor, it is necessary to augment the previous force equation with terms describing the interaction with the charge. In the long-wavelength limit of the electric field E, the force equations then become

$$\begin{aligned} -m\omega^2 u_{2r} &= m(d^2u_{2r}/dt^2) = \alpha(u_{2r+1} + u_{2r-1} - 2u_{2r}) + e^*E \\ &= \alpha(e^{i2qa} + 1)u_{2r-1} - 2\alpha u_{2r} + e^*E \end{aligned} \tag{2.8}$$

and

$$\begin{aligned} -M\omega^2 u_{2r+1} &= M(d^2u_{2r+1}/dt^2) = \alpha(u_{2r+2} + u_{2r} - 2u_{2r+1}) - e^*E \\ &= \alpha(1 + e^{-i2qa})u_{2r+2} - 2\alpha u_{2r+1} - e^*E. \end{aligned} \tag{2.9}$$

Regarding the phonon displacements, in the long-wavelength limit there is no need to distinguish between the different sites for a given mass type since all atoms of the same mass are displaced by the same amount. In this limit, $q \to 0$. Denoting the displacements on even-numbered sites by u_1 and those on odd-numbered sites by u_2, in the long-wavelength limit the force equations reduce to

$$-m\omega^2 u_1 = 2\alpha(u_2 - u_1) + e^*E \tag{2.10}$$

and

$$-M\omega^2 u_2 = 2\alpha(u_1 - u_2) - e^*E. \tag{2.11}$$

Adding these equations demonstrates that $-m\omega^2 u_1 - M\omega^2 u_2 = 0$ and it is clear that $mu_1 = -Mu_2$; thus

$$-m\omega^2 u_1 = 2\alpha\left(-\frac{m}{M}u_1 - u_1\right) + e^*E \tag{2.12}$$

and

$$-M\omega^2 u_2 = 2\alpha\left(u_1 + \frac{m}{M}u_1\right) - e^*E; \tag{2.13}$$

accordingly,

$$-(\omega^2 - \omega_0^2)u_1 = e^*E/m \tag{2.14}$$

and

$$-(\omega^2 - \omega_0^2)u_2 = -e^*E/M \tag{2.15}$$

where $\omega_0^2 = 2\alpha(1/m + 1/M)$ is the resonant frequency squared, in the absence of Coulomb effects; that is, for $e^* = 0$. The role of e^* in shifting the phonon frequency will be discussed further in the next section.

Clearly, the electric polarization P produced by such a polar diatomic lattice is given by

$$P = \frac{Ne^*u}{\epsilon(\infty)} = \frac{Ne^*(u_1 - u_2)}{\epsilon(\infty)} = \frac{1}{\epsilon(\infty)}\frac{Ne^{*2}}{(\omega_0^2 - \omega^2)}\left(\frac{1}{m} + \frac{1}{M}\right)E, \tag{2.16}$$

where $u = u_1 - u_2$, N is the number of pairs per unit volume, and e^* is as defined previously. This equation may be rewritten to show that it describes a driven oscillator:

$$(\omega_0^2 - \omega^2)u = e^*\left(\frac{1}{m} + \frac{1}{M}\right)E. \tag{2.17}$$

2.3.2 Displacement patterns for phonons

As discussed in subsection 2.3.1, in the limit $q \to 0$ the displacements, u_1 and u_2, of the optical modes satisfy $-mu_1 = Mu_2$ and the amplitudes of the two types of mass have opposite signs. That is, for the optical modes the atoms vibrate out of phase, and so with their center of mass fixed. For the acoustic modes, the maximum frequency is $(2\alpha/M)^{1/2}$. This maximum frequency occurs at the zone edge so that, near the center of the zone, ω is much less than $(2\alpha/M)^{1/2}$. From subsection 2.3.1, the ratio A_2/A_1 may be expressed as

$$\frac{A_2}{A_1} = \frac{2\alpha\cos qa}{2\alpha - M\omega^2} = \frac{2\alpha - m\omega^2}{2\alpha\cos qa}, \tag{2.18}$$

and it is clear that the ratio of the displacement amplitudes is approximately equal to unity for acoustic phonons near the center of the Brillouin zone. Thus, in contrast to the optical modes, the acoustic modes are characterized by in-phase motion of

the different masses m and M. Typical mode patterns for zone-center acoustic and optical modes are depicted in Figures 2.3(a), (b). The transverse modes are illustrated here since the longitudinal modes are more difficult to depict graphically. The higher-frequency optical modes involve out-of-plane oscillations of adjacent ions, while the lower-frequency acoustic modes are characterized by motion of adjacent ions on the same sinusoidal curve.

2.3.3 Polaritons

In the presence of a transverse electric field, transverse optical (TO) phonons of a polar medium couple strongly to the electric field. When the wavevectors and frequencies of the electric field are in resonance with those of the TO phonon, a coupled phonon–photon field is necessary to describe the system. The quantum of this coupled field is known as the polariton. The analysis of subsection 2.3.1 may be generalized to apply to the case of transverse displacements. In particular, for a transverse field E, the oscillator equation takes the form

$$(\omega_{\mathrm{TO}}^2 - \omega^2)P = \frac{Ne^{*2}}{\epsilon(\infty)}\left(\frac{1}{m} + \frac{1}{M}\right)E, \tag{2.19}$$

where ω_0^2 of subsection 2.3.1 has been designated $\omega_{\mathrm{TO}}^2 = 2\alpha(1/m + 1/M)$ since the resonant frequency in the absence of Coulomb effects, $e^{*2} = 0$, corresponds to

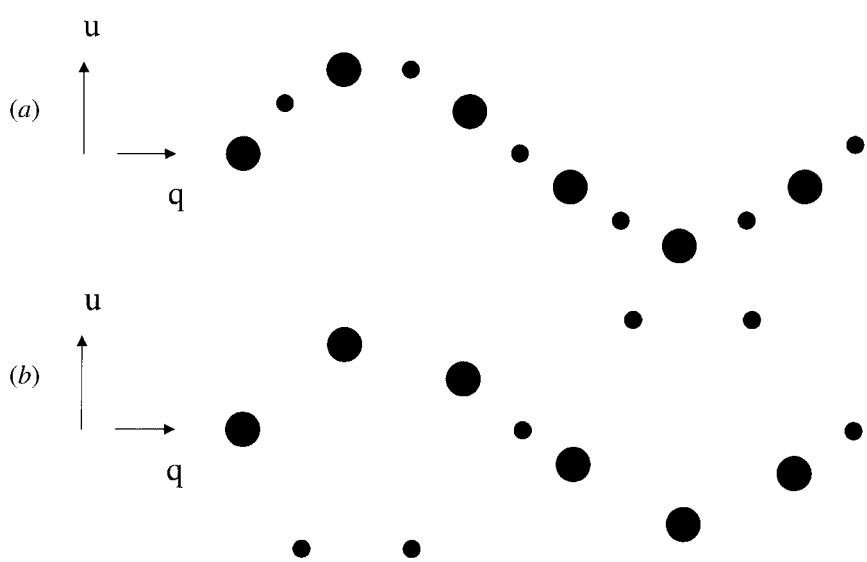

Figure 2.3. Transverse displacements of heavy ions (large disks) and light ions (small disks) for (a) transverse acoustic modes, and (b) transverse optical modes propagating in the q-direction.

the transverse optical frequency. As will become apparent later in this section, the LO phonon frequency squared differs from the TO phonon frequency squared by an amount proportional to e^{*2}.

According to the electromagnetic wave equation, $\partial^2 D/\partial t^2 = c^2\nabla^2 E$, where $D = E + 4\pi P$, the dispersion relation describing the coupling of the field E of the electromagnetic wave to the electric polarization P of the TO phonon is

$$c^2q^2E = \omega^2(E + 4\pi P) \tag{2.20}$$

or, alternatively,

$$4\pi\omega^2 P = (c^2q^2 - \omega^2)E, \tag{2.21}$$

where waves of the form $e^{i(qr-\omega t)}$ have been assumed. The driven oscillator equation and the electromagnetic wave equation have a joint solution when the determinant of the coefficients of the fields E and P vanishes,

$$\begin{vmatrix} \omega^2 - c^2q^2 & 4\pi\omega^2 \\ \dfrac{Ne^{*2}}{\epsilon(\infty)}\left(\dfrac{1}{m} + \dfrac{1}{M}\right) & -(\omega_{\mathrm{TO}}^2 - \omega^2) \end{vmatrix} = 0 \tag{2.22}$$

At $q = 0$, there are two roots: $\omega = 0$ and

$$\omega^2 = \omega_{\mathrm{TO}}^2 + 4\pi\frac{Ne^{*2}}{\epsilon(\infty)}\left(\frac{1}{m} + \frac{1}{M}\right) = \omega_{\mathrm{LO}}^2. \tag{2.23}$$

The dielectric function $\epsilon(\omega)$ is then given by

$$\begin{aligned}\epsilon(\omega) &= \frac{D(\omega)}{E(\omega)} = 1 + \frac{4\pi P_{\mathrm{e}}(\omega)}{E(\omega)} + \frac{4\pi P(\omega)}{E(\omega)} \\ &= 1 + \frac{4\pi P_{\mathrm{e}}(\omega)}{E(\omega)} + \frac{4\pi}{(\omega_{\mathrm{TO}}^2 - \omega^2)}\frac{Ne^{*2}}{\epsilon(\infty)}\left(\frac{1}{m} + \frac{1}{M}\right),\end{aligned} \tag{2.24}$$

where the polarization due to the electronic contribution, $P_{\mathrm{e}}(\omega)$, has been included as well as the polarization associated with the ionic contribution, $P(\omega)$.

As is customary, the dielectric constant due to the electronic response is denoted by

$$\epsilon(\infty) = 1 + \frac{4\pi P_{\mathrm{e}}(\omega)}{E(\omega)}, \tag{2.25}$$

and it follows that

$$\epsilon(\omega) = \epsilon(\infty) + \frac{4\pi}{(\omega_{\mathrm{TO}}^2 - \omega^2)}\frac{Ne^{*2}}{\epsilon(\infty)}\left(\frac{1}{m} + \frac{1}{M}\right). \tag{2.26}$$

The so-called static dielectric constant $\epsilon(0)$ is then given by

$$\epsilon(0) = \epsilon(\infty) + \frac{4\pi}{\omega_{\mathrm{TO}}^2}\frac{Ne^{*2}}{\epsilon(\infty)}\left(\frac{1}{m} + \frac{1}{M}\right). \tag{2.27}$$

From these last two results it follows straightforwardly that

$$\begin{aligned}\epsilon(\omega) &= \epsilon(\infty) + \frac{[\epsilon(0) - \epsilon(\infty)]\omega_{\mathrm{TO}}^2}{(\omega_{\mathrm{TO}}^2 - \omega^2)} \\ &= \epsilon(\infty) + \frac{\epsilon(0) - \epsilon(\infty)}{1 - \omega^2/\omega_{\mathrm{TO}}^2}.\end{aligned} \tag{2.28}$$

From electromagnetic theory it is known that the dielectric function $\epsilon(\omega)$ must vanish for any longitudinal electromagnetic disturbance to propagate. Accordingly, the frequency of the LO phonons, ω_{LO}, must be such that $\epsilon(\omega_{\mathrm{LO}}) = 0$; from the last equation, this condition implies that

$$\epsilon(\omega_{\mathrm{LO}}) = 0 = \epsilon(\infty) + \frac{\epsilon(0) - \epsilon(\infty)}{1 - \omega_{\mathrm{LO}}^2/\omega_{\mathrm{TO}}^2} \tag{2.29}$$

or, equivalently,

$$\omega_{\mathrm{LO}} = \left[\frac{\epsilon(0)}{\epsilon(\infty)}\right]^{1/2}\omega_{\mathrm{TO}}. \tag{2.30}$$

It then follows that

$$\begin{aligned}\epsilon(\omega) &= \epsilon(\infty) + \frac{\epsilon(0) - \epsilon(\infty)}{1 - \omega^2/\omega_{\mathrm{TO}}^2} = \epsilon(\infty) + \frac{(\omega_{\mathrm{LO}}/\omega_{\mathrm{TO}})^2\epsilon(\infty) - \epsilon(\infty)}{1 - \omega^2/\omega_{\mathrm{TO}}^2} \\ &= \epsilon(\infty)\left\{1 + \frac{(\omega_{\mathrm{LO}}/\omega_{\mathrm{TO}})^2 - 1}{1 - \omega^2/\omega_{\mathrm{TO}}^2}\right\} \\ &= \epsilon(\infty)\left(\frac{\omega_{\mathrm{TO}}^2 - \omega^2}{\omega_{\mathrm{TO}}^2 - \omega^2} + \frac{\omega_{\mathrm{LO}}^2 - \omega_{\mathrm{TO}}^2}{\omega_{\mathrm{TO}}^2 - \omega^2}\right) \\ &= \epsilon(\infty)\frac{\omega_{\mathrm{LO}}^2 - \omega^2}{\omega_{\mathrm{TO}}^2 - \omega^2},\end{aligned} \tag{2.31}$$

or alternatively

$$\frac{\epsilon(\omega)}{\epsilon(\infty)} = \frac{\omega_{\mathrm{LO}}^2 - \omega^2}{\omega_{\mathrm{TO}}^2 - \omega^2}. \tag{2.32}$$

In the special case where $\omega = 0$, this relation reduces to the celebrated Lyddane–Sachs–Teller relationship

$$\frac{\epsilon(0)}{\epsilon(\infty)} = \frac{\omega_{\mathrm{LO}}^2}{\omega_{\mathrm{TO}}^2}. \tag{2.33}$$

When $\omega = \omega_{\mathrm{LO}}$ the dielectric constant vanishes, $\epsilon(\omega_{\mathrm{LO}}) = 0$; as stated above, this condition is familiar from electromagnetics as a requirement for the propagation

of a longitudinal electromagnetic wave. That is, a longitudinal electromagnetic wave propagates only at frequencies where the dielectric constant vanishes; accordingly, ω_{LO} is identified as the frequency of the LO phonon. From the relation

$$\omega_{\mathrm{TO}}^2 + 4\pi \frac{Ne^{*2}}{\epsilon(\infty)}\left(\frac{1}{m} + \frac{1}{M}\right) = \omega_{\mathrm{LO}}^2,$$

it follows that $\omega_{\mathrm{TO}} = \omega_{\mathrm{LO}}$ for zone-center phonons in materials with $e^* = 0$; this is just as observed in non-polar materials such as silicon. In polar materials such as GaAs there is a gap between ω_{TO} and ω_{LO}, associated with the Coulomb energy density arising from e^*. When $\omega = \omega_{\mathrm{TO}}$, $\epsilon(\omega_{\mathrm{TO}})^{-1} = 0$ and the pole in $\epsilon(\omega)$ reflects the fact that electromagnetic waves with the frequency of the TO phonon are absorbed. Throughout the interval $(\omega_{\mathrm{TO}}, \omega_{\mathrm{LO}})$, $\epsilon(\omega)$ is negative and electromagnetic waves do not propagate.

2.3.4 Macroscopic theory of polar modes in cubic crystals

As was apparent in subsections 2.3.1 and 2.3.3, polar-optical phonon vibrations produce electric fields and electric polarization fields that may be described in terms of Maxwell's equations and the driven-oscillator equations. Loudon (1964) advocated a model of optical phonons based on these macroscopic fields that has had great utility in describing the properties of optical phonons in so-called uniaxial crystals such as würtzite crystals. The Loudon model for uniaxial crystals will be developed more fully in Chapters 3 and 7. In this section, the concepts underlying the Loudon model will be discussed in the context of cubic crystals.

From the pair of Maxwell's equations,

$$\nabla \times \mathbf{E} + \frac{1}{c}\frac{\partial \mathbf{B}}{\partial t} = 0 \qquad \text{and} \qquad \nabla \times \mathbf{B} - \frac{1}{c}\frac{\partial \mathbf{D}}{\partial t} = \mathbf{J}, \tag{2.34}$$

it follows that

$$\nabla \times (\nabla \times \mathbf{E}) + \frac{1}{c}\frac{\partial (\nabla \times \mathbf{B})}{\partial t} = \nabla(\nabla \cdot \mathbf{E}) - \nabla^2 \mathbf{E} + \frac{1}{c^2}\frac{\partial^2 \mathbf{D}}{\partial^2 t} = 0, \tag{2.35}$$

where the source current, $\mathbf{J}$, has been taken to equal zero. Then since $\nabla \cdot \mathbf{D} = \nabla \cdot \mathbf{E} + 4\pi \nabla \cdot \mathbf{P} = 4\pi\rho = 0$, it follows that

$$-4\pi \nabla(\nabla \cdot \mathbf{P}) - \nabla^2 \mathbf{E} + \frac{1}{c^2}\frac{\partial^2 \mathbf{E}}{\partial^2 t} + 4\pi \frac{1}{c^2}\frac{\partial^2 \mathbf{P}}{\partial^2 t} = 0. \tag{2.36}$$

Assuming that P and E both have spatial and time dependences of the form $e^{i(\mathbf{q}\cdot\mathbf{r} - \omega t)}$, this last result takes the form

$$\mathbf{E} = \frac{-4\pi[\mathbf{q}(\mathbf{q} \cdot \mathbf{P}) - \omega^2 \mathbf{P}/c^2]}{q^2 - \omega^2/c^2}. \tag{2.37}$$

The condition $\mathbf{q}\cdot\mathbf{P}=0$ corresponds to the transverse wave; in this case,

$$\mathbf{E}=\frac{-4\pi\omega^2\mathbf{P}/c^2}{q^2-\omega^2/c^2}. \tag{2.38}$$

From Appendix A, $\mathbf{E}$ and $\mathbf{P}$ are also related through

$$\mathbf{P}=\frac{1}{4\pi}\left\{\frac{[\epsilon(0)-\epsilon(\infty)]\omega_{\mathrm{TO}}^2}{\omega_{\mathrm{TO}}^2-\omega^2}+[\epsilon(\infty)-1]\right\}\mathbf{E}; \tag{2.39}$$

thus

$$\frac{q^2-\omega^2/c^2}{\omega^2/c^2}=\frac{[\epsilon(0)-\epsilon(\infty)]\omega_{\mathrm{TO}}^2}{\omega_{\mathrm{TO}}^2-\omega^2}+[\epsilon(\infty)-1], \tag{2.40}$$

or, equivalently,

$$\frac{q^2c^2}{\omega^2}=\frac{\omega_{\mathrm{TO}}^2\epsilon(0)-\omega^2\epsilon(\infty)}{\omega_{\mathrm{TO}}^2-\omega^2}. \tag{2.41}$$

For longitudinal waves, $\mathbf{q}\cdot\mathbf{P}=qP$, so that $\mathbf{q}=(q/P)\mathbf{P}$, and it follows that

$$\begin{aligned}\mathbf{E}&=\frac{4\pi\omega^2\mathbf{P}/c^2}{q^2-\omega^2/c^2}-\frac{4\pi qP\mathbf{q}}{q^2-\omega^2/c^2}\\&=\frac{4\pi\omega^2\mathbf{P}/c^2}{q^2-\omega^2/c^2}-\frac{4\pi q^2\mathbf{P}}{q^2-\omega^2/c^2}\\&=\frac{4\pi}{q^2-\omega^2/c^2}\left(\frac{\omega^2}{c^2}-q^2\right)\mathbf{P}\\&=-4\pi\mathbf{P}.\end{aligned} \tag{2.42}$$

Then

$$\begin{aligned}\mathbf{P}&=\frac{1}{4\pi}\left\{\frac{[\epsilon(0)-\epsilon(\infty)]\omega_{\mathrm{TO}}^2}{\omega_{\mathrm{TO}}^2-\omega^2}+[\epsilon(\infty)-1]\right\}\mathbf{E}\\&=-\left\{\frac{[\epsilon(0)-\epsilon(\infty)]\omega_{\mathrm{TO}}^2}{\omega_{\mathrm{TO}}^2-\omega^2}+[\epsilon(\infty)-1]\right\}\mathbf{P}\end{aligned} \tag{2.43}$$

or, equivalently,

$$\omega=\omega_{\mathrm{TO}}\left[\frac{\epsilon(0)}{\epsilon(\infty)}\right]^{1/2}=\omega_{\mathrm{LO}},$$

and the Lyddane–Sachs–Teller relation is recovered once again! In Chapter 3, we shall return to the Loudon model to describe uniaxial crystals of the würtzite type.

Chapter 3

Phonons in bulk würtzite crystals

Next when I cast mine eyes and see that brave vibration, each way free; O how that glittering taketh me.
Robert Herrick, 1648

3.1 Basic properties of phonons in würtzite structure

The GaAlN-based semiconductor structures are of great interest in the electronics and optoelectronics communities because they possess large electronic bandgaps suitable for fabricating semiconductor lasers with wavelengths in the blue and ultraviolet as well as electronic devices designed to work at elevated operating temperatures. These III-V nitrides occur in both zincblende and würtzite structures. In this chapter, the würtzite structures will be considered rather than the zincblende structures, since the treatment of the phonons in these würtzite structures is more complicated than for the zincblendes. Throughout the remainder of this book, phonon effects in nanostructures will be considered for both the zincblendes and würtzites. This chapter focuses on the basic properties of phonons in bulk würtzite structures as a foundation for subsequent discussions on phonons in würtzite nanostructures.

The crystalline structure of a würtzite material is depicted in Figure 3.1. As in the zincblendes, the bonding is tetrahedral. The würtzite structure may be generated from the zincblende structure by rotating adjacent tetrahedra about their common bonding axis by an angle of 60 degrees with respect to each other. As illustrated in Figure 3.1, würtzite structures have four atoms per unit cell.

The total number of normal vibrational modes for a unit cell with s atoms in the basis is $3s$. As for cubic materials, in the long-wavelength limit there are three acoustic modes, one longitudinal and two transverse. Thus, the total number of optical modes in the long-wavelength limit is $3s - 3$. These optical modes must, of course, appear with a ratio of transverse to longitudinal optical modes of two.

The numbers of the various long-wavelength modes are summarized in Table 3.1.

For the zincblende case, $s = 2$ and there are six modes: one LA, two TA, one LO and two TO. For the würtzite case, $s = 4$ and there are 12 modes: one LA, two TA, three LO and six TO. In the long-wavelength limit the acoustic modes are simple translational modes. The optical modes for a würtzite structure are depicted in Figure 3.2.

From Figure 3.2 it is clear that the A_1 and E_1 modes will produce large electric polarization fields when the bonding is ionic. Such large polarization fields result in strong carrier–optical-phonon scattering. These phonon modes are known as infrared active. As we shall see in Chapter 5, the fields associated with these infrared modes may be derived from a potential describing the carrier–phonon interaction of

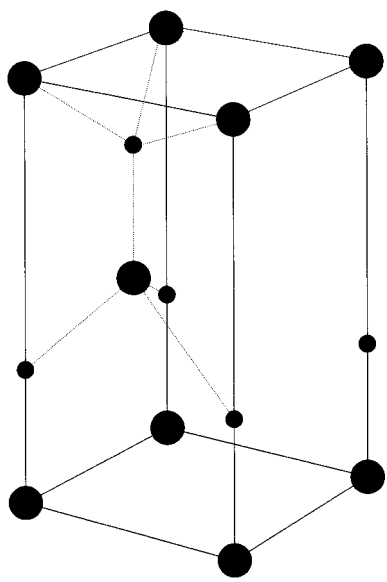

Figure 3.1. Unit cell of the hexagonal würtzite crystal.

Table 3.1. Phonon modes associated with a unit cell having s atoms in the basis.

Type of mode	Number of modes
Longitudinal acoustic (LA)	1
Transverse acoustic (TA)	2
All acoustic modes	3
Longitudinal optical (LO)	$s - 1$
Transverse optical (TO)	$2s - 2$
All optical modes	$3s - 3$
All modes	$3s$

such modes. In Chapter 5, this carrier–phonon interaction potential will be identified as the Fröhlich interaction. The dispersion relations for the 12 phonon modes of the würtzite structure are depicted in Figure 3.3.

The low-frequency behavior of these modes near the Γ point makes it apparent that three of these 12 modes are acoustic modes. This behavior is, of course, consistent with the number of acoustic modes identified in Table 3.1.

3.2 Loudon model of uniaxial crystals

As discussed in subsection 2.3.4, Loudon (1964) advanced a model for uniaxial crystals that provides a useful description of the longitudinal optical phonons in würtzite crystals. In Loudon's model of uniaxial crystals such as GaN or AlN, the angle between the c-axis and q is denoted by θ, and the isotropic dielectric constant of the cubic case is replaced by dielectric constants for the directions parallel and perpendicular to the c-axis, $\epsilon_{\parallel}(\omega)$ and $\epsilon_{\perp}(\omega)$ respectively. That is,

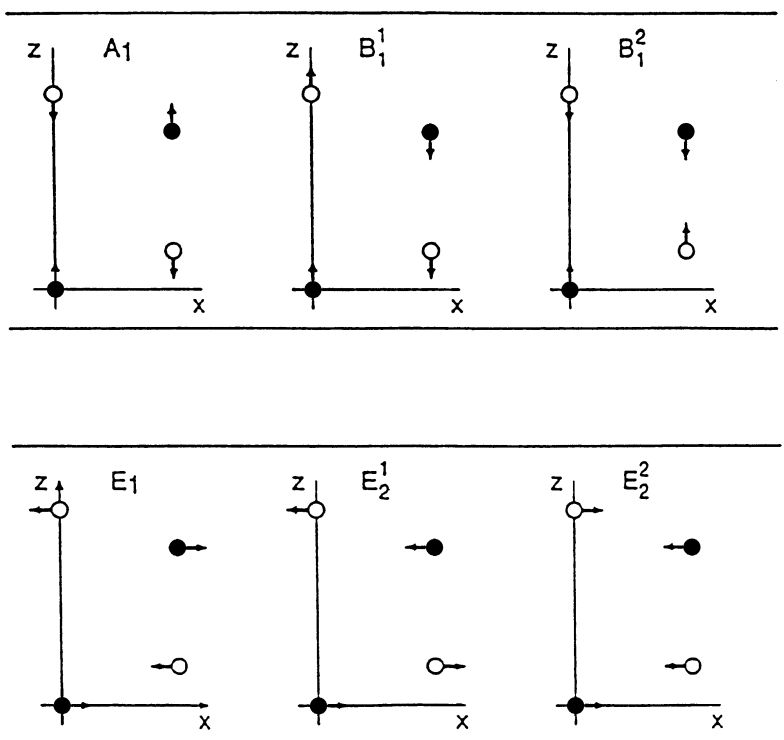

Figure 3.2. Optical phonons in würtzite structure. From Gorczyca *et al.* (1995), American Physical Society, with permission.

$$\epsilon(\omega) = \begin{pmatrix} \epsilon_\perp(\omega) & 0 & 0 \\ 0 & \epsilon_\perp(\omega) & 0 \\ 0 & 0 & \epsilon_\parallel(\omega) \end{pmatrix} \tag{3.1}$$

with

$$\epsilon_\perp(\omega) = \epsilon_\perp(\infty)\frac{\omega^2 - \omega_{\mathrm{LO},\perp}^2}{\omega^2 - \omega_{\mathrm{TO},\perp}^2} \qquad \text{and} \qquad \epsilon_\parallel(\omega) = \epsilon_\parallel(\infty)\frac{\omega^2 - \omega_{\mathrm{LO},\parallel}^2}{\omega^2 - \omega_{\mathrm{TO},\parallel}^2}, \tag{3.2}$$

as required by the Lyddane–Sachs–Teller relation. The c-axis is frequently taken to be in the z-direction and the dielectric constant is then sometimes labeled by the z-coordinate; that is, $\epsilon_\parallel(\omega) = \epsilon_z(\omega)$. Figure 3.4 depicts the two dielectric constants for GaN as well as those for AlN.

In such a uniaxial crystal, there are two types of phonon wave: (a) ordinary waves where for any θ both the electric field **E** and the polarization **P** are perpendicular to the c-axis and **q** simultaneously, and (b) extraordinary waves, for which the orientation of **E** and **P** with respect to **q** and the c-axis is more complicated. As discussed in subsection 2.3.4, the ordinary wave has E_1 symmetry, is transverse, and is polarized in the $\perp$-plane. There are two extraordinary waves, one associated with the $\perp$-polarized vibrations and having A_1 symmetry and the other associated with $\parallel$-polarized vibrations and having E_1 symmetry. For $\theta = 0$, one of these modes is the A_1(LO) mode and the other is the E_1(TO) mode. As θ varies between 0 and $\pi/2$, these modes evolve to the A_1(TO) and E_1(TO) modes respectively. For values of θ intermediate between 0 and $\pi/2$ they are mixed and do not have purely LO or

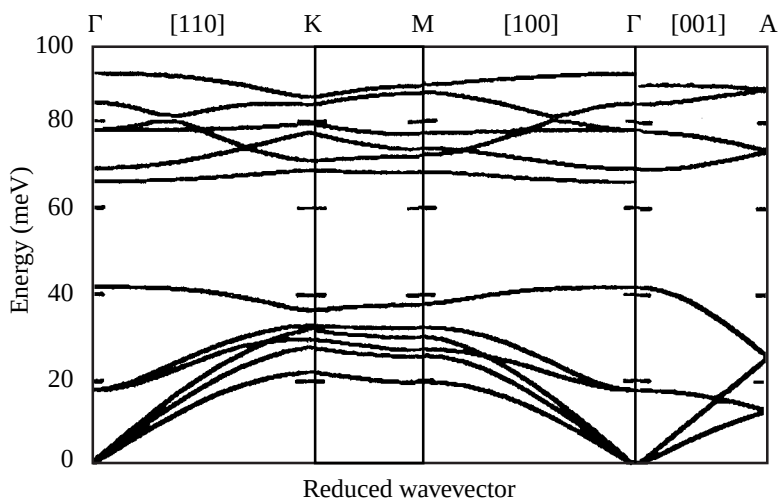

Figure 3.3. Phonon dispersion curves for GaN crystal of würtzite structure. From Nipko *et al.* (1998), American Institute of Physics, with permission.

TO character or A_1 or E_1 symmetry (Loudon, 1964). For würtzite structures at the Γ point, it will be obvious in Chapter 7 that only three of the nine optical phonon modes, the $A_1(Z)$ and $E_1(X, Y)$ modes, produce significant carrier–optical-phonon scattering rates. These are the so-called infrared-active modes. For the case of würtzite structures, Loudon's model of uniaxial crystals is based upon generalizing Huang's equations, equations (A.8) and (A.9) of Appendix A, and the relationship of subsection 2.3.4, equation (2.43). Specifically, for each of these equations there is a set of two more equations, one in terms of quantities along the c-axis and the other in terms of quantities perpendicular to the c-axis:

$$(\omega_{\mathrm{TO},\perp}^2 - \omega^2)\mathbf{u}_\perp = \left(\frac{V}{4\pi\mu N}\right)^{1/2} \sqrt{\epsilon_\perp(0) - \epsilon_\perp(\infty)}\, \omega_{\mathrm{TO},\perp}\mathbf{E}_\perp, \tag{3.3}$$

$$(\omega_{\mathrm{TO},\parallel}^2 - \omega^2)\mathbf{u}_\parallel = \left(\frac{V}{4\pi\mu N}\right)^{1/2} \sqrt{\epsilon_\parallel(0) - \epsilon_\parallel(\infty)}\, \omega_{\mathrm{TO},\parallel}\mathbf{E}_\parallel, \tag{3.4}$$

$$\mathbf{P}_\perp = \left(\frac{\mu N}{4\pi V}\right)^{1/2} \sqrt{\epsilon_\perp(0) - \epsilon_\perp(\infty)}\, \omega_{\mathrm{TO},\perp}\mathbf{u}_\perp + \left[\frac{\epsilon_\perp(\infty) - 1}{4\pi}\right]\mathbf{E}_\perp, \tag{3.5}$$

$$\mathbf{P}_\parallel = \left(\frac{\mu N}{4\pi V}\right)^{1/2} \sqrt{\epsilon_\parallel(0) - \epsilon_\parallel(\infty)}\, \omega_{\mathrm{TO},\parallel}\mathbf{u}_\parallel + \left[\frac{\epsilon_\parallel(\infty) - 1}{4\pi}\right]\mathbf{E}_\parallel, \tag{3.6}$$

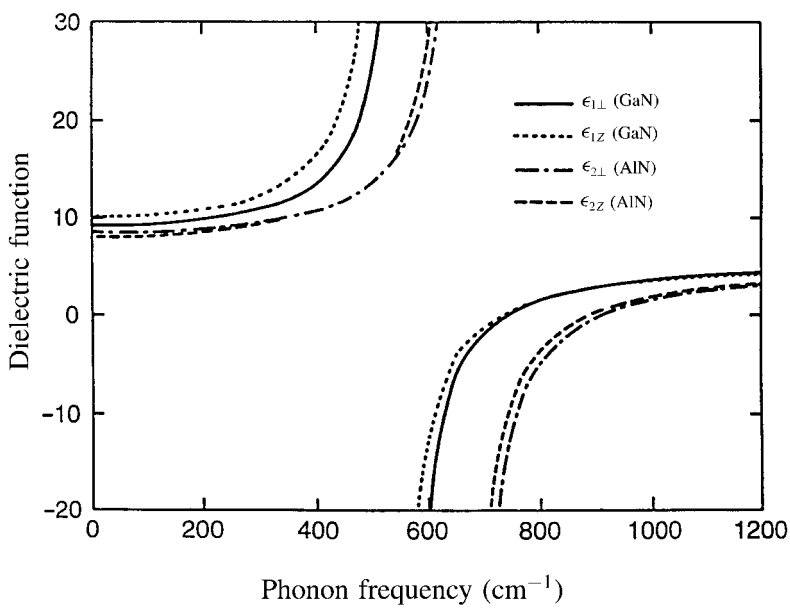

Figure 3.4. Dielectric constants for GaN, $\epsilon_{1\perp}$(GaN) and ϵ_{1z}(GaN), and for AlN, $\epsilon_{2\perp}$(AlN) and ϵ_{2z}(AlN). From Lee *et al.* (1998), American Physical Society, with permission.